

# Blending Heteroskedasticity and Sign Restrictions: Restoring Rotation Invariance

Dawis Kim

November 7, 2025

## Abstract

Under sign restrictions, structural vector autoregressive models (SVARs) are *rotation invariant*: any orthogonal rotation of the shocks yields an observationally equivalent model. Introducing heteroskedasticity breaks this symmetry—volatility shifts tilt the likelihood toward particular rotations, biasing inference. I develop a Bayesian SVAR with stochastic volatility and sign restrictions (SVAR–SVSR) that integrates heteroskedasticity with economically motivated constraints—sign, narrative, elasticity-bound, and zero restrictions—while restoring rotation invariance. The method jointly rotates the contemporaneous impact matrix and the regime-specific variance matrices, ensuring that posterior inference depends only on the imposed economic restrictions rather than arbitrary likelihood tilts. In applications to oil-market, monetary-policy, and optimism shocks, the approach preserves the informational content of heteroskedasticity, tightens credible sets, and yields economically interpretable impulse responses.

## 1 Introduction

In SVAR, identification depends on assumptions that single out one rotation of the model’s innovations as the true set of structural shocks. Under standard sign restrictions, the likelihood is *rotation invariant*—any orthogonal rotation of the shocks fits the data equally well. Introducing heteroskedasticity breaks this invariance: the likelihood favors specific rotations even when they are economically equivalent, creating what I call an *accidental likelihood tilt*. This paper develops a Bayesian framework that restores rotation invariance, allowing heteroskedasticity and sign restrictions to work together coherently.

Economists often analyze the propagation of shocks using VAR models. Identifying shocks relies on flexible strategies such as sign restrictions, narrative restrictions, or external instruments. Since Uhlig

(2005), sign restrictions have become especially popular: they are easy to apply and yield clear economic interpretations, but they typically deliver set identification and face issues such as weak or mis-identified shocks and ambiguous inference (Wolf, 2020).

Another strand of the literature exploits heteroskedasticity as a source of identification.<sup>1</sup> Volatility shifts can, in principle, reveal valuable information. In practice, however, identification may be weak in finite samples, and the labeling of shocks often remains unresolved. Section 2 reviews both strategies in more detail.

I formalize this idea through a Bayesian SVAR with stochastic volatility and sign restrictions (SVAR-SVSR) that coherently integrates the two identification approaches. Heteroskedasticity is modeled through predefined volatility regimes, following Brunnermeier et al. (2021), while sign restrictions are imposed on impulse responses using a common orthogonal matrix across regimes, as in Rubio-Ramírez et al. (2010). While Baumeister and Hamilton (2015) restrict identification by truncating priors on the contemporaneous matrix, sign restrictions on impulse responses allow researchers to flexibly search for structural shocks across horizons.

The key insight is that combining sign restrictions with heteroskedasticity is not straightforward. When volatility shifts are present, the likelihood is no longer invariant to orthogonal rotations (Arias et al., 2024). I address this by drawing orthogonal matrices from the uniform (Haar) distribution, rotating both the contemporaneous matrix and the regime-specific variances, and sampling the structural parameters with a Metropolis–Hastings step. For each draw, I compute impulse responses and retain only the rotations that satisfy the sign restrictions. Restoring rotation invariance ensures that only the sign restrictions guide inference, rather than the likelihood giving unfair weight to certain rotations.

I illustrate the framework in three applications—two that parallel Carriero et al. (2024) and one that incorporates zero restrictions. Restoring rotation invariance produces effects similar to those documented by Carriero et al. (2024), but the posterior credible sets are generally tighter and often take a more economically interpretable shape. In the monetary-policy VAR, heteroskedasticity sharpens inference on the effects of policy shocks, reducing uncertainty about their impact on output and inflation. In the oil-market VAR, it aligns the responses of economic activity with theoretical priors by producing negative output effects following oil-specific demand shocks. In the optimism-shock VAR, the integration of heteroskedasticity and sign restrictions further tightens the credible sets.

The paper’s contributions are fourfold.

---

<sup>1</sup>See, among others, Rigobon (2003), Lanne et al. (2010), and Brunnermeier et al. (2021).

First, I develop a coherent framework that combines heteroskedasticity and sign restrictions without breaking rotation invariance. Recent work has attempted to merge the two approaches but has overlooked this problem (Lütkepohl and Netšunajev, 2014; Carriero et al., 2024). Lanne and Luoto (2020) recognize the issue and address it by restricting the orthogonal matrix to signed permutations, but this solution is less general. In contrast, my method restores rotation invariance while allowing the full set of orthogonal rotations by jointly rotating both the contemporaneous matrix and the structural variances.

Second, the approach samples directly in structural space and imposes sign restrictions on the entire sequence of impulse responses, not just contemporaneous effects, while remaining consistent with heteroskedasticity. Most existing work instead samples from the reduced-form posterior, which confines priors to the inverse-Wishart–normal family. For example, Lütkepohl and Netšunajev (2014) and Carriero et al. (2024) draw in reduced-form space and impose sign restrictions only ex post. Even when researchers move to structural space, as in Lanne and Luoto (2020) or Braun (2023), the restrictions are typically limited to the impact matrix rather than the full IRFs.

Third, the framework accommodates additional restrictions—narrative information, elasticity bounds, and zero restrictions—without loss of coherence. Finally, the applications demonstrate that enforcing internal consistency across identification schemes can tighten credible sets and deliver more robust conclusions.

## Related Literature

This paper contributes to three strands of research. First, sign-restriction identification pioneered by Uhlig (2005) and extended by Rubio-Ramírez et al. (2010) and others provides flexible yet set-identified inference. Second, heteroskedasticity-based identification (Rigobon, 2003; Lanne et al., 2010; Brunnermeier et al., 2021) exploits variance shifts for point identification but often leaves the economic labeling unresolved. Third, recent work attempts to merge these approaches (Lütkepohl and Netšunajev, 2014; Lanne and Luoto, 2020; Carriero et al., 2024), though these methods generally overlook the loss of rotation invariance. This paper unifies the two strategies by restoring that invariance and embedding narrative, elasticity, and zero restrictions within a coherent Bayesian framework.

## 2 Discussions on Identification Issues

### 2.1 Sign Restrictions

Researchers use two main strategies to impose sign restrictions in SVARs. The first is to place informative priors directly on structural parameters, as in [Baumeister and Hamilton \(2015\)](#). The second, which is more common in practice, draws uniformly from orthonormal rotation matrices that transform the reduced-form VAR into structural models consistent with the restrictions ([Rubio-Ramírez et al., 2010](#); [Uhlig, 2005](#)).

The prior-based method integrates economic beliefs into a Bayesian framework, but it does not guarantee that impulse responses satisfy the required sign patterns over the full horizon. This shortcoming becomes important when the dynamics of the responses matter as much as their contemporaneous signs.

The rotation-based method instead imposes restrictions directly on the impulse responses. It samples orthogonal matrices  $Q \in \mathbb{O}(n)$  and accepts only those that generate responses consistent with the restrictions. Under standard assumptions—Gaussian likelihood and homoskedastic errors—this procedure exploits rotation invariance: rotating  $(A_0, A_+)$  by any orthogonal  $Q$  leaves the joint prior and likelihood unchanged. As a result, posterior inference does not depend on the particular rotation chosen, as long as the restrictions are met. However, this approach delivers only set identification rather than point identification. The accepted draws span a range of admissible models, which often leads to wider credible intervals and greater uncertainty in inference.

### 2.2 Heteroskedasticity (Stochastic Volatility)

A different identification strategy exploits time variation in the volatility of structural shocks. This idea, first developed by [Rigobon \(2003\)](#) and extended by [Lanne et al. \(2010\)](#), treats volatility shifts not as a nuisance but as useful information for identifying the impact matrix.

Volatility changes are common in macro and financial data. Ignoring them can distort estimation, as outliers may drive spurious revisions to dynamics ([Clark, 2011](#)). In contrast, sharp and well-structured variance shifts can help identify structural shocks ([Sims, 2020](#); [Lewis, 2021](#)).

There are two main ways to model heteroskedasticity. One is to divide the sample into predefined regimes with distinct volatility patterns, often tied to historical episodes. This regime-switching approach, used by [Brunnermeier et al. \(2021\)](#), is transparent and robust: identification remains valid even if break dates are not perfectly accurate, as long as the relative variance shifts are large enough ([Sims, 2020](#); [Lewis, 2021](#)).

The other strategy lets the data determine regimes through Hidden Markov Models, often estimated in a Bayesian framework ([Sims and Zha, 2006](#)). This method adds flexibility but also complexity. It can be sensitive to prior choices and may suffer from label switching or overfitting, especially in short samples.

Even when theoretically sound, volatility-based identification may still be weak in practice. Small or poorly aligned variance shifts can make it difficult to separate shocks. In those cases, blending heteroskedasticity with economically motivated restrictions—such as sign restrictions—can substantially improve identification ([Sims, 2020](#); [Carriero et al., 2024](#)). Still, even predefined regimes face challenges: ambiguous regime labeling or weak volatility separation can complicate interpretation.

In the next section, I develop a framework that combines sign restrictions with heteroskedasticity while addressing the technical issue of rotation invariance.

### 3 Combining Heteroskedasticity with Sign Restrictions

#### 3.1 Empirical Model

I build on the structural VAR model in [Rubio-Ramírez et al. \(2010\)](#), allowing for heteroskedastic shocks. The baseline specification is given by:

$$y_t' A_0 = C + \sum_{j=1}^p y_{t-j}' A_j + \epsilon_t' \quad (1)$$

where  $y_t$  is an  $n \times 1$  vector of endogenous variables observed over time periods  $t \in \mathcal{T} := \{1, \dots, T\}$ . The matrix  $A_0$  captures contemporaneous relationships among the variables, while  $(A_j)_{j=1}^p$  are  $n \times n$  matrices of lagged coefficients. The vector  $C$  contains constant terms, and  $\epsilon_t$  is an  $n \times 1$  vector of structural shocks, which are assumed to be mutually and serially uncorrelated. The number of lags is denoted by  $p$ .

The key identifying assumption in this model is that while the dynamic coefficients  $(A_j)_{j=1}^p$  remain constant over time, the variances of the structural shocks vary across distinct periods—or regimes. I assume:

$$E[\epsilon_t \epsilon_t'] = \Lambda_{m(t)} \quad (2)$$

where  $m(\cdot) : \mathcal{T} \rightarrow \mathcal{M}$  is a regime mapping function that assigns each time period  $t$  to a regime  $m \in \mathcal{M} := \{1, \dots, M\}$ . Each  $\Lambda_{m(t)}$  is a diagonal covariance matrix representing the regime-specific variances of the structural shocks<sup>2</sup>.

---

<sup>2</sup>To account for large outlier shocks, I allow the structural shocks to exhibit additional idiosyncratic variance, following

Following [Brunnermeier et al. \(2021\)](#), I normalize the variances across regimes by imposing:

$$\frac{1}{M} \sum_{m=1}^M \lambda_{i,m} = 1 \quad \forall i \in \{1, \dots, n\} \quad (3)$$

where  $\lambda_{i,m}$  denotes the  $i$ th diagonal element of  $\Lambda_m$ . This normalization ensures that, for each variable, the average variance of its structural shock across regimes is equal to one. Intuitively, this setup allows the model to capture changes in the relative size of shocks across time, without altering the way the system responds to them.

For notational convenience, I rewrite the model in compact form as:

$$y_t' A_0 = x_t' A_+ + \epsilon_t' \quad (4)$$

where  $x_t$  is a  $n(np + 1)$  matrix containing lagged values of  $Y$  and a column of ones (to capture the constant). The reduced-form representation implied by the structural model (4) is:

$$y_t' = x_t' A_+ A_0^{-1} + u_t' \quad (5)$$

where  $u_t' = \epsilon_t' A_0^{-1}$ , and  $E[u_t u_t'] = A_0^{-1'} \Lambda_{m(t)} A_0^{-1}$ .

Recent empirical work combines sign restrictions with heteroskedasticity ([Lütkepohl and Netšunajev, 2014](#); [Lanne and Luoto, 2020](#); [Braun, 2023](#); [Carriero et al., 2024](#)). The idea is to use both methods in a complementary way: variance shifts across regimes can narrow the set of admissible structural matrices, while sign restrictions (and related tools such as narrative restrictions, elasticity bounds, or zero restrictions) provide the economic interpretation that purely statistical identification lacks. In principle, this blend harnesses the statistical power of heteroskedasticity while preserving the flexibility of sign restrictions.

One common implementation builds directly on the procedure of [Rubio-Ramírez et al. \(2010\)](#): draw orthogonal rotation matrices  $Q$  from the uniform distribution, impose sign restrictions via rejection sampling, and evaluate the likelihood under the heteroskedastic model. This delivers a clean extension of the standard sign-restricted SVAR framework, enriched with information from time-varying volatility.

These blended approaches are appealing, but they overlook a critical technical point: once heteroskedasticity is introduced, the likelihood is no longer invariant to orthogonal rotations. The next subsection formalizes

---

[Brunnermeier et al. \(2021\)](#). Appendix A provides further details.

this breakdown.

### 3.2 Rotation Invariance and Its Breakdown

**Definition 1** (Rotation Invariance). A likelihood (or posterior) is rotation-invariant if, for any orthogonal matrix  $Q \in \mathbb{O}(n)$ , rotating the structural parameters  $(A_0, A_+)$  into  $(A_0Q, A_+Q)$  leaves the distribution unchanged. Formally,  $p(Y | A_0, A_+) = p(Y | A_0Q, A_+Q), \forall Q \in \mathbb{O}(n)$ .

Rotation invariance means inference depends only on the space spanned by the shocks, not on how we label or rotate them. Under homoskedastic Gaussian errors,  $\varepsilon_t \sim \mathcal{N}(0, \Lambda)$ ,  $\Lambda = \sigma^2 I_n$ , the reduced-form likelihood satisfies this property. For any orthogonal  $Q$ ,  $p(Y | A_0, A_+) = p(Y | A_0Q, A_+Q)$ , so orthogonal rotations of  $(A_0, A_+)$  produce observationally equivalent models (Rubio-Ramírez et al., 2010). When the prior on  $(A_0, A_+)$  is also rotation-invariant—such as the Sims–Zha reference prior or any prior that factors through the reduced form  $(B, \Sigma_u)$ —the posterior inherits this invariance.

This property breaks down under regime-specific heteroskedasticity,  $\varepsilon_t \sim \mathcal{N}(0, \Lambda_{m(t)})$  with  $\Lambda_m \notin I_n$  (Arias et al., 2024).

**Proposition 1** (Failure of rotation invariance under heteroskedasticity). *Consider a SVAR with structural shocks  $\varepsilon_t \sim \mathcal{N}(0, \Lambda_{m(t)})$ , where each  $\Lambda_{m(t)}$  is diagonal and at least one regime has two distinct diagonal entries ( $\Lambda_{m(t)} \notin I_n$ ). Let  $u_t = A_0^{-1} \varepsilon_t$ , so that  $u_t \sim \mathcal{N}(0, \Sigma_t)$  with  $\Sigma_t = A_0^{-1} \Lambda_{m(t)} A_0^{-1'}$ . For any orthogonal matrix  $Q \in \mathbb{O}(n)$ , define the rotated impact matrix  $\tilde{A}_0 = A_0 Q$  and the implied covariance  $\tilde{\Sigma}_t = A_0^{-1} Q' \Lambda_{m(t)} Q A_0^{-1'}$ . Then the reduced-form Gaussian likelihood is not rotationally invariant:*

$$p(Y | A_0, A_+, \Lambda_{m(\cdot)}) \neq p(Y | A_0Q, A_+Q, \Lambda_{m(\cdot)})$$

for all  $Q$  outside the commuting set  $\{Q : Q' \Lambda_{m(t)} Q = \Lambda_{m(t)} \forall t\}$ . In particular, full rotation invariance holds if and only if  $\Lambda_{m(t)} \propto I_n$  in every regime.

*Proof.* See Arias et al. (2024) for a detailed argument. The likelihood depends only on the sequence of covariances  $\{\Sigma_t\}_t$ . Invariance requires  $\tilde{\Sigma}_t = \Sigma_t$  for all  $t$ , which is equivalent to

$$Q' \Lambda_{m(t)} Q = \Lambda_{m(t)} \quad \forall t.$$

If  $\Lambda_{m(t)}$  is diagonal with unequal variances, the only orthogonal matrices satisfying this condition are block

rotations or signed permutations within groups of equal variances. Generic rotations do not commute with  $\Lambda_{m(t)}$ , so  $\tilde{\Sigma}_t \neq \Sigma_t$  in at least one regime, and the likelihood changes. When every  $\Lambda_{m(t)}$  is proportional to the identity, however, the condition holds for all  $Q$ , restoring full rotation invariance.  $\square$

[Carriero et al. \(2024\)](#) propose a combined approach that uses both heteroskedasticity and sign restrictions, but they do not address the breakdown of rotation invariance in the likelihood. By contrast, [Arias et al. \(2024\)](#) emphasize this problem and show that once heteroskedasticity enters, the standard uniform prior over  $Q$  no longer delivers a flat posterior over the identified set. This breakdown matters for Bayesian applications, where inference relies on the assumption that both the likelihood and the posterior remain invariant to rotation. When invariance fails, posterior draws lose a clear interpretation, and researchers must carefully assess the plausibility and robustness of the resulting impulse responses.

### 3.3 Restoring Rotation Invariance

To restore rotation invariance under regime-specific heteroskedasticity, I rotate every component of the structural VAR system with a common orthogonal matrix  $Q \in \mathbb{O}(n)$ . The transformation applies to the contemporaneous impact matrix  $A_0$ , the autoregressive coefficients  $A_+$ , and the regime-dependent structural variance matrices  $\Lambda_{m(t)}$ .

**Proposition 2** (Restoring rotation invariance of likelihood under heteroskedasticity). *Let the structural shocks follow  $\varepsilon_t \sim \mathcal{N}(0, \Lambda_{m(t)})$ , with possibly regime-dependent and non-spherical variances  $\Lambda_{m(t)}$ . Define the structural parameters  $(A_0, A_+, \Lambda_m)$ , and suppose we apply a common orthogonal transformation  $Q \in \mathbb{O}(n)$  to all components of the system:*

$$(A_0, A_+, \Lambda_m) \mapsto (A_0 Q, A_+ Q, Q' \Lambda_m Q).$$

*Then the reduced-form Gaussian likelihood is rotation-invariant under this transformation:*

$$p(Y | A_0, A_+, \Lambda_m) = p(Y | A_0 Q, A_+ Q, Q' \Lambda_m Q).$$

*Proof.* The reduced-form covariance in regime  $m$  is  $\Sigma_t = A_0^{-1} \Lambda_{m(t)} A_0^{-1'}$ . Under the joint transformation, the

rotated covariance is

$$\tilde{\Sigma}_t = (A_0 Q)^{-1} (Q' \Lambda_{m(t)} Q) (A_0 Q)^{-1'} = Q' A_0^{-1} Q Q' \Lambda_{m(t)} Q Q' A_0^{-1'} Q.$$

Because  $Q' Q = I$ , this simplifies to

$$\tilde{\Sigma}_t = A_0^{-1} \Lambda_{m(t)} A_0^{-1'} = \Sigma_t.$$

□

Proposition 2 shows that we can restore rotation invariance in heteroskedastic SVARs by rotating both the structural parameters  $(A_0, A_+)$  and the structural variance matrices  $\Lambda_{m(t)}$  with the same transformation. The likelihood remains invariant under this joint rotation, but the prior on  $\Lambda_{m(t)}$  does not. Most applications of heteroskedasticity, including this one, assume that  $\Lambda_{m(t)}$  is diagonal and place priors directly on its diagonal elements. Any orthogonal rotation  $Q' \Lambda_{m(t)} Q$  generally produces a full (non-diagonal) matrix, which breaks prior invariance. Even so, the prior on  $\Lambda_{m(t)}$  plays only a minor role relative to the likelihood. As a result, the posterior remains driven primarily by the data, and the main effect comes from restoring rotation invariance at the likelihood level.

Table 1 summarizes the key differences between this paper and [Carriero et al. \(2024\)](#) regarding rotation invariance.

**Table 1:** Comparison of Rotation Invariance: This Paper vs. [Carriero et al. \(2024\)](#)

Property	This Paper	<a href="#">Carriero et al. (2024)</a>
Rotation Invariance of Likelihood	✓	✗
Rotation Invariance of Prior Density	✗	✓
Transformation Applied to $\Lambda_{m(t)}$	$Q' \Lambda_{m(t)} Q$	$\Lambda_{m(t)}$
Treatment of $A_0, A_+$	Rotated as $A_0 Q, A_+ Q$	Rotated as $A_0 Q, A_+ Q$

### 3.4 Impact Matrix under Rotation

Rotations of the shock basis only relabel the structural shocks; they do not change the reduced-form fit of the VAR. This subsection shows that result formally.

Let the regime-specific structural covariance be  $\Lambda_m$  and define the (time-0) impact matrix

$$S_m = \Lambda_m^{1/2} A_0^{-1}.$$

Impulse responses at horizon  $h$  are  $\text{IRF}(h) = S_m R(h)$ , where  $R(h)$  is the standard VAR recursion.

Now consider an orthogonal change of shock basis  $Q \in \mathbb{O}(n)$ . Apply the joint rotation to the contemporaneous and variance blocks:  $A_0^{-1} \mapsto Q'A_0^{-1}$ , and  $\Lambda_m \mapsto Q'\Lambda_m Q$ . The rotated (time-0) impact becomes

$$\tilde{S}_m = (Q'\Lambda_m Q)^{1/2} (Q'A_0^{-1}) = (Q'\Lambda_m^{1/2} Q) (Q'A_0^{-1}) = Q'\Lambda_m^{1/2} A_0^{-1} = Q' S_m.$$

Hence the rotation  $Q$  acts by right-multiplying  $S_m$ : it rotates the *columns* (shock directions) identically in every regime. Impulse responses transform accordingly:

$$\text{IRF}(h) \mapsto \tilde{S}_m R(h) = Q' S_m R(h)$$

This reparameterization leaves the reduced-form fit unchanged in every regime. In other words, rotating the shocks only relabels the structural innovations—it does not alter the dynamics  $R(h)$  or the implied reduced-form covariances.

### 3.5 SVAR-SVSR Gibbs Sampler

---

#### SVAR-SVSR Algorithm

1. **Initialization.** Initialize the parameter vector  $x_0$  at its posterior mode. Estimate the inverse Hessian matrix  $H$  by numerically maximizing the unnormalized log-posterior in equation (11). Discard the first 1,000 draws as burn-in to ensure convergence.
  
2. **Metropolis–Hastings with Sign Restrictions.** For each iteration  $j$ , draw a proposal  $x^* \sim \mathcal{N}(x_{j-1}, c \cdot H)$ , where  $c = 0.1$  targets a 30% acceptance rate. Compute:

$$\alpha^j = \min \left\{ 1, \frac{P[\Upsilon_t | \Upsilon_0, A_+, x^*, \theta_3] \cdot P[x^*]}{P[\Upsilon_t | \Upsilon_0, A_+, x_{j-1}, \theta_3] \cdot P[x_{j-1}]} \right\}.$$

- (a) If  $x^*$  is accepted, extract  $A_0^*$ ,  $\{\Lambda_m^*\}_{m=1}^M$ , and compute  $A_+^*$  as in Appendix B.2.

(b) Attempt to find a valid rotation  $Q \in \mathbb{O}(n)$  such that:

- Draw  $Q$  from the Haar distribution (uniformly over orthogonal matrices).
- Rotate the structural parameters:

$$\tilde{A}_0 = Q \cdot A_0^*, \quad \tilde{\Lambda}_m = Q \Lambda_m^* Q^\top.$$

- Construct regime-specific impact matrices using:

$$\text{IRF basis at time } 0 : A_0^{*-1} \cdot \sqrt{\Lambda_m^*} \cdot Q^\top,$$

where  $\sqrt{\cdot}$  denotes the matrix square root.

- Check whether the impulse responses satisfy the sign restrictions in all regimes.

(c) If a valid  $Q$  is found within 1000 trials, accept the draw and retain the rotated system  $(\tilde{A}_0, \tilde{\Lambda}_m)$ . Otherwise, reject  $x^*$  and return to Step 2.

---

3. **Update Volatility States.** If using stochastic volatility, draw each  $\xi_{i,t}^{(j)}$  from its inverse-gamma posterior conditional on  $u_{i,t}^{(j)}$ , using a degrees of freedom parameter (e.g., 5.7).

---

4. **Repeat Sampling.** Iterate Steps 2–3 until 3,000 posterior draws are collected.

---

The Gibbs sampling algorithm with stochastic volatility and sign restrictions (SVAR–SVSR) builds on [Brunnermeier et al. \(2021\)](#). It adds a sign-restriction step but keeps the volatility and state updates unchanged. Unlike [Carriero et al. \(2024\)](#), who work in reduced-form space under a Uniform–Normal–Inverse-Wishart prior and then draw  $Q$  from the Haar measure to enforce signs by rejection (using the Waggoner–Zha sampler for equation-by-equation coefficients), SVAR–SVSR operates directly in structural space.

At each iteration, I propose  $(A_0, \{A_j\}_{j=1}^P, \{\Lambda_m\}_{m=1}^M)$  via a Metropolis–Hastings step. Given a rotation  $Q \in \mathbb{O}(n)$ , I apply the joint orthogonal reparameterization

$$A_0^{-1} \mapsto Q' A_0^{-1}, \quad \Lambda_m \mapsto Q' \Lambda_m Q,$$

which preserves the rotation invariance of the likelihood.

I then compute impulse responses using  $S_m = \Lambda_m^{1/2} A_0^{-1}$ , so that  $\tilde{S}_m = Q' S_m$ . I retain only those rotations  $Q$  that satisfy the imposed sign restrictions. This structural-space MH step guarantees that accepted draws remain consistent with the heteroskedastic posterior while producing the same reduced-form fit. By contrast,

[Carriero et al. \(2024\)](#) evaluate the likelihood in reduced-form space and rely on uniform  $Q$  with rejection to impose signs.

## 4 Empirical Evaluation of the SVAR-SVSR Model

In this section, I extend the methodology by combining sign restrictions with additional identifying assumptions, always in the presence of heteroskedasticity. I consider three applications: (i) sign restrictions with elasticity bounds (oil market, [Kilian and Murphy \(2012\)](#)), (ii) sign restrictions with narrative restrictions (monetary policy shocks, [Antolín-Díaz and Rubio-Ramírez \(2018\)](#)), and (iii) sign restrictions with zero restrictions (optimism shocks, [Arias et al. \(2018\)](#)). Each of these variants is straightforward to implement within the SVAR-SVSR sampling framework.

The first two applications follow [Carriero et al. \(2024\)](#), whereas the third—combining sign, zero, and heteroskedasticity restrictions—is novel to this paper.

### 4.1 Sign Restrictions with Elasticity Bounds and Heteroskedasticity

[Kilian and Murphy \(2012\)](#) uses plausible magnitude bounds on impulse responses to tighten the wide set of models admitted under standard sign restrictions. This strategy sharpens the identification of demand and supply shocks in the oil market. The VAR(24) with constant includes three variables:  $\Delta q_t$  (oil production growth),  $y_t$  (global activity), and  $p_t$  (real oil price). Table 2 summarizes the sign restrictions and elasticity bounds.

**Table 2:** Sign and Elasticity Restrictions for Oil Market SVAR

	$\Delta q_t$ (Oil Supply)	$y_t$ (Global Activity)	$p_t$ (Real Oil Price)	Elasticity bound
<b>Oil Supply Shock</b>	–	–	+	
<b>Aggregate Demand Shock</b>	+	+	+	$\frac{\Delta q_t}{p_t} \leq 0.0258$
<b>Oil-Specific Demand Shock</b>	+	–	+	$\frac{\Delta q_t}{p_t} \leq 0.0258$

I estimate the model using normal priors on the elements of  $A_0$  and on the coefficients in  $A_+$ , without additional assumptions such as Minnesota priors, sum-of-coefficients priors, or dummy-initial-observation priors. This setup aligns with the flat priors on reduced-form parameters in [Kilian and Murphy \(2012\)](#) and [Carriero et al. \(2024\)](#). The sample covers January 1971 to December 2015, extended by [Antolín-Díaz and](#)

Rubio-Ramírez (2018)<sup>3</sup>.

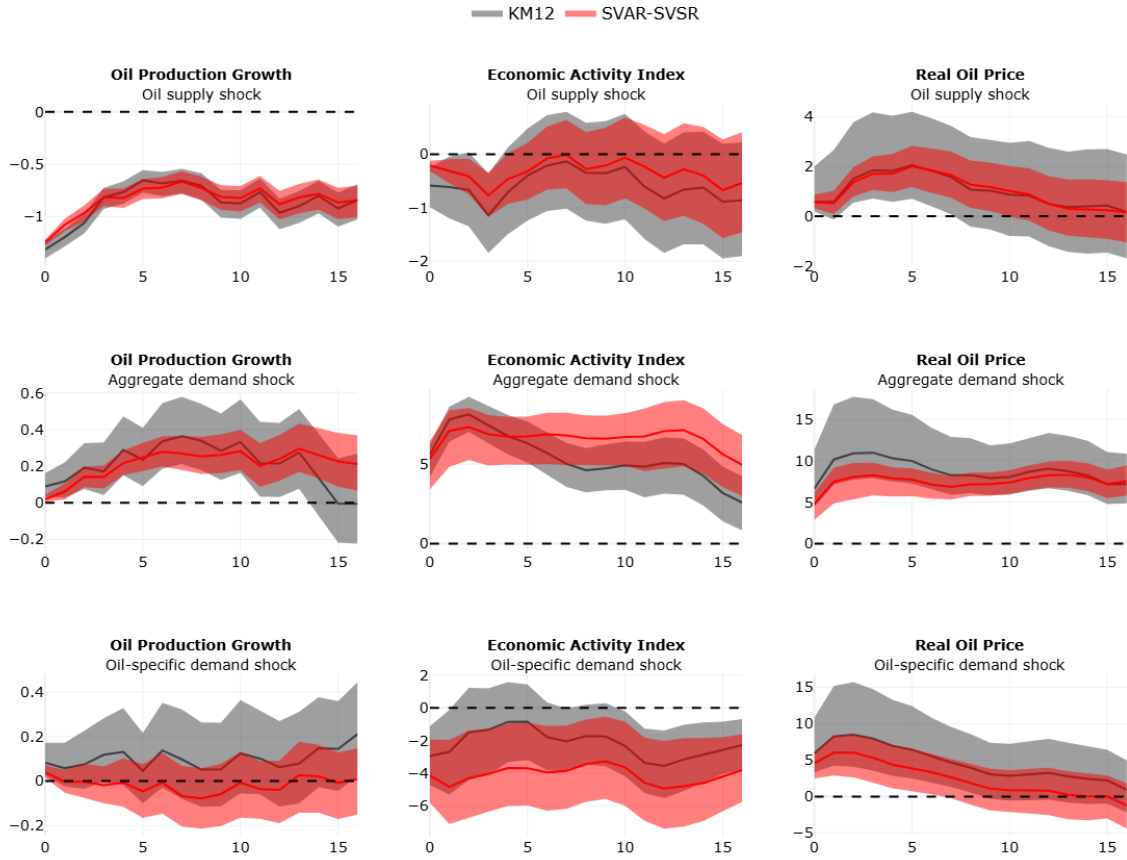


**Figure 1:** Impulse response comparisons of SVAR-SVSR with Kilian and Murphy (2012).

**Notes:** KM12 (gray) corresponds to the SVAR in Kilian and Murphy (2012), and SVAR-SVSR (red) indicates the heteroskedastic model. The predefined regimes in SVAR-SVSR are January 1971–December 1989, January 1990–December 2007, and January 2008–December 2015.

Figure 1 compares impulse responses (IRFs) from SVAR-SVSR (red) with those from KM12 (gray)<sup>4</sup>.

The SVAR-SVSR regimes follow Carriero et al. (2024), motivated by Brunnermeier et al. (2021): January 1971–December 1989, January 1990–December 2007, and January 2008–December 2015.

For oil supply and aggregate demand shocks, SVAR-SVSR produces IRFs that closely track KM12 but with much tighter error bands. For oil-specific demand shocks, however, the results align more closely with economic intuition. SVAR-SVSR shows oil production responses concentrated around zero and global activity responses that remain negative across horizons. In contrast, KM12 report wider error bands that overlap

<sup>3</sup>The dataset is available on Juan Antolin-Diaz's website.

<sup>4</sup>I obtain the KM12 IRFs using SVAR-SVSR without heteroskedasticity, i.e. by setting  $M = 1$ . The gray IRFs therefore differ slightly from those in Kilian and Murphy (2012), which are sampled in reduced-form space, but remain very similar.

with positive global activity responses at some horizons, while [Carriero et al. \(2024\)](#) find strictly positive responses across longer periods. Thus, SVAR-SVSR delivers both tighter inference and a more economically plausible interpretation of global activity's response to oil-specific demand shocks<sup>5</sup>.

I compare SVAR-SVSR with and without structural variance in Appendix C.1 to assess the practical importance of variance rotation in restoring likelihood rotation invariance in the sign+elasticity-bound+heteroskedastic model. Figure 5 shows that both models deliver nearly identical median IRFs. SVAR-SVSR with variance rotation yields only marginally tighter credible intervals at very early horizons for a few variables.

## 4.2 Sign Restrictions with Narrative Restrictions and Heteroskedasticity

[Antolín-Díaz and Rubio-Ramírez \(2018\)](#) combines sign restrictions with narrative information from historical episodes to sharpen the identification of monetary policy shocks. This approach builds on [Uhlig \(2005\)](#), who relied only on sign restrictions. I adopt the same var{12} model without a constant term, which includes real output, the GDP deflator, a commodity price index, total reserves, non-borrowed reserves, and the federal funds rate. Table 3 summarizes the sign restrictions and narrative information.

**Table 3:** Sign and Narrative Restrictions for Monetary Policy Shock

	GDP Deflator	Commodity Prices	Non-borrowed Reserves	Federal Funds Rate
<b>Monetary Policy Shock</b>	– (6m)	– (6m)	– (6m)	+ (6m)
<b>Narrative:</b> Shock was positive and the main driver of the federal funds rate increase in September 1979 (Volcker disinflation).				

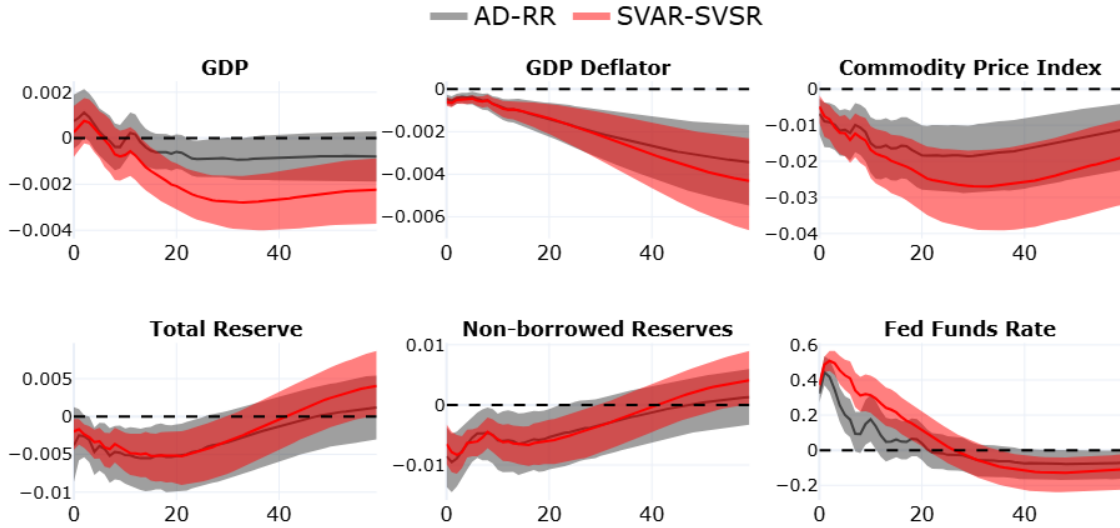
I estimate the model using normal priors on the elements of  $A_0$  and on the coefficients in  $A_+$ , without additional assumptions such as Minnesota priors, sum-of-coefficients priors, or dummy-initial-observation priors. This setup aligns with the flat priors on reduced-form parameters in [Antolín-Díaz and Rubio-Ramírez \(2018\)](#) and [Carriero et al. \(2024\)](#). The estimation sample runs from January 1965 to November 2007<sup>6</sup>.

Figure 2 compares impulse responses (IRFs) from SVAR-SVSR (red) with those from AD-RR (gray)<sup>7</sup>. The SVAR-SVSR regimes follow [Brunnermeier et al. \(2021\)](#), who identify monetary policy shocks through heteroskedasticity: January 1965–December 1972, January 1973–September 1979, October 1979–December

<sup>5</sup>A negative response of global activity to oil-specific demand shocks is more consistent with economic intuition. These shocks reflect precautionary demand for oil, often driven by concerns about future supply disruptions. They raise oil prices without boosting demand for other goods and services, effectively acting as a tax on oil importers and dampening global output.

<sup>6</sup>The dataset is available on Juan Antolín-Díaz's website.

<sup>7</sup>I obtain the AD-RR IRFs using SVAR-SVSR without heteroskedasticity, i.e. by setting  $M = 1$ . The gray IRFs therefore differ slightly from those in [Antolín-Díaz and Rubio-Ramírez \(2018\)](#), which are sampled in reduced-form space, but remain very similar.



**Figure 2:** Impulse response comparisons of SVAR-SVSR with [Antolín-Díaz and Rubio-Ramírez \(2018\)](#).

**Notes:** AD-RR (gray) corresponds to the SVAR in [Antolín-Díaz and Rubio-Ramírez \(2018\)](#), and SVAR-SVSR (red) indicates the heteroskedastic model. The predefined regimes in SVAR-SVSR are January 1965–December 1972, January 1973–September 1979, October 1979–December 1982, January 1983–December 1989, and January 1990–November 2007.

1982, January 1983–December 1989, and January 1990–November 2007.

The SVAR-SVSR results closely track AD-RR but with much tighter error bands for Total Reserves and Non-Borrowed Reserves. SVAR-SVSR also shows a more pronounced and persistent decline in commodity prices following a monetary policy shock<sup>8</sup>. Moreover, SVAR-SVSR delivers strictly negative responses of real GDP a few months after the shock, consistent with the expected contractionary effect of monetary tightening. By contrast, AD-RR error bands remain close to zero even at longer horizons. These results are in line with the findings of [Carriero et al. \(2024\)](#).

Figure 6 in Appendix C.2 compares SVAR-SVSR with and without structural variance. Both models yield nearly identical median IRFs, but SVAR-SVSR with variance rotation produces substantially tighter credible intervals across all variables. This contrast highlights that restoring rotation invariance is more consequential in the sign+ narrative + heteroskedastic setting than in the sign+ elasticity-bound + heteroskedastic model.

<sup>8</sup>A fall in commodity prices following a contractionary monetary policy shock is consistent with the demand channel of monetary transmission. Higher interest rates reduce consumption and investment, lowering demand for raw materials and energy. By contrast, a negative productivity shock would typically put upward pressure on commodity prices by tightening supply. Thus, the decline in commodity prices supports the interpretation that the identified shock is a monetary policy shock rather than a productivity disturbance.

The stronger effect of variance rotation in the sign+narrative+heteroskedastic model reflects the fact that narrative restrictions and heteroskedasticity both extract information directly from the data. Narrative restrictions operate through reduced-form residuals tied to historical episodes, while variance rotation preserves the likelihood information coming from heteroskedasticity. Taken together, these mechanisms reinforce one another, which makes rotation invariance more consequential in this setting. By contrast, elasticity bounds rely more on theory than on data, so variance rotation has a weaker effect.

### 4.3 Sign Restrictions with Zero Restrictions and Heteroskedasticity

[Rubio-Ramírez et al. \(2010\)](#); [Arias et al. \(2018\)](#) propose a method to construct the orthogonal matrix  $Q$  that jointly imposes zero restrictions and sign restrictions on impulse responses. As shown in Subsection 3.4, under heteroskedasticity the time-0 impact matrix—after rotating both the contemporaneous matrix  $A_0$  and the structural variances  $\Lambda_{m(t)}$ —becomes

$$A_0^{-1} \cdot \Lambda_{m(t)}^{1/2},$$

while the subsequent impulse response dynamics remain unchanged. This property makes it straightforward to extend the zero-restriction approach of [Rubio-Ramírez et al. \(2010\)](#); [Arias et al. \(2018\)](#) to the heteroskedastic SVAR-SVSR setting. The orthogonal matrix  $Q$  must satisfy

$$Z_j \cdot R(h) \cdot A_0^{-1} \cdot \Lambda_{m(t)}^{1/2} \cdot q_j = 0,$$

where  $Z_j$  selects the zero restrictions,  $R(h)$  is the dynamic response operator, and  $q_j$  is the  $j$ -th column of  $Q$ .

Building on this theoretical advantage, I estimate a VAR{4} with a constant term, including adjusted TFP, stock prices, consumption, the real interest rate, and hours worked. Table 4 summarizes the zero and sign restrictions.

**Table 4:** Sign-Zero Restrictions for Optimism Shock

	Adjusted TFP	Stock Prices
<b>Optimism Shock</b>	0	+

I estimate the model using normal priors on the elements of  $A_0$  and on the coefficients in  $A_+$ , without additional assumptions such as Minnesota priors, sum-of-coefficients priors, or dummy-initial-observation priors. This setup aligns with the flat priors on reduced-form parameters in [Arias et al. \(2018\)](#) and [Carriero et al. \(2018\)](#).

et al. (2024). The estimation sample runs from the first quarter of 1955 to the last quarter of 2010<sup>9</sup>.

The sign–zero identification based on the orthogonal matrix shows that the optimism shock does not generate any meaningful expansionary effects on the economy. This finding contrasts with the argument in Mountford and Uhlig (2009), who used a penalty function approach to impose combined sign and zero restrictions.

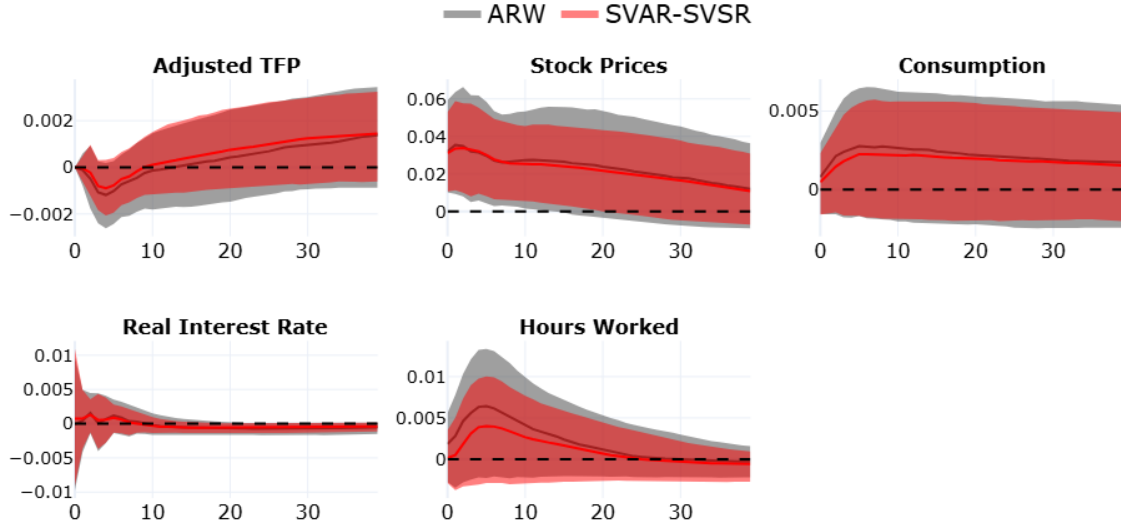


**Figure 3:** Impulse response comparisons of SVAR-SVSR with Arias et al. (2018).

**Notes:** ARW (gray) corresponds to the SVAR in Arias et al. (2018), and SVAR-SVSR (red) indicates the heteroskedastic model. The predefined regimes in SVAR-SVSR are Q1 1955–Q4 1972, Q1 1973–Q4 1989, and Q1 1990–Q4 2010.

Figure 3 compares impulse responses (IRFs) from SVAR-SVSR (red) with those from ARW (gray)<sup>10</sup>. The SVAR-SVSR regimes follow Brunnermeier et al. (2021): Q1 1955–Q4 1972, Q1 1973–Q4 1989, and Q1 1990–Q4 2010. The results are not sensitive to the exact choice or number of regimes, as long as at least three regimes are used.

Adding heteroskedasticity to the sign+zero restrictions produces tighter error bands for all variables. The median responses of consumption and hours worked become closer to zero at most horizons, implying that the optimism shock does not generate meaningful expansionary effects on the economy, reinforcing the findings in Arias et al. (2018).

Figure 7 in Appendix C.3 compares SVAR-SVSR with and without rotating structural variance. Both

<sup>9</sup>The dataset is available on Juan Antolin-Diaz's website.

<sup>10</sup>I obtain the ARW IRFs using SVAR-SVSR without heteroskedasticity, i.e. by setting  $M = 1$ . The gray IRFs therefore differ slightly from those in Arias et al. (2018), which are sampled in reduced-form space, but remain very similar.

models yield nearly identical median IRFs but joint rotation of  $A_0$  and  $\Lambda_m$  has narrower error bands, indicating that restoring rotation invariance has effect of reducing uncertainty in the sign+zero+heteroskedastic setting.

## 5 Robustness: Penalty Function for Prior Invariance

As shown in Subsection 3.3, the likelihood remains rotation-invariant under the joint transformation of  $(A_0, A_+, \Lambda_{m(t)})$ . The prior on  $\Lambda_{m(t)}$ , however, does not. Most applications assume  $\Lambda_{m(t)}$  is diagonal and place priors directly on its diagonal elements. Any orthogonal rotation  $Q' \Lambda_{m(t)} Q$  typically produces a full (non-diagonal) matrix, breaking prior invariance.

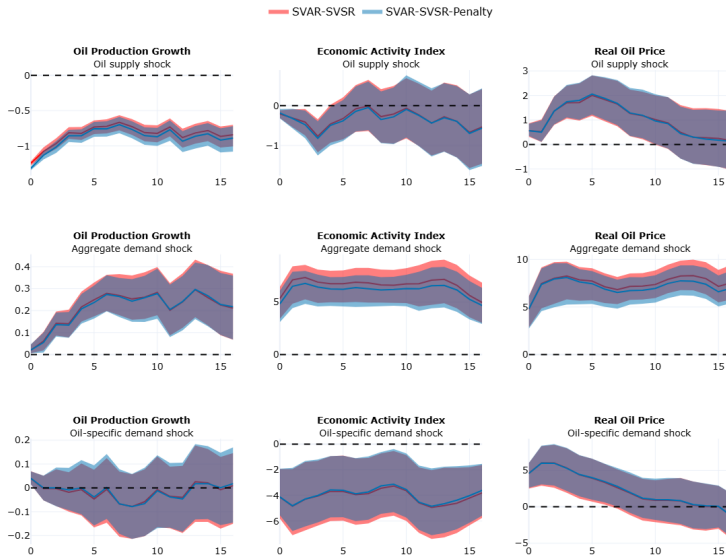
To address this, I use a *penalty function*. I accept a draw of  $Q$  only if every diagonal element of  $\Lambda_{m(t)}$  is larger than the maximum off-diagonal entry, scaled by the penalty parameter. This condition encourages approximate diagonality and, with it, a degree of prior invariance.

The approach has limitations. Selecting the penalty weight is delicate: a large value overconstrains the model, while a small value leaves off-diagonal elements unchecked. The penalty also complicates the posterior surface, which can reduce the stability of Gibbs sampling. Even when satisfied, the rotated  $\Lambda_{m(t)}$  remains only approximately diagonal, complicating interpretation.

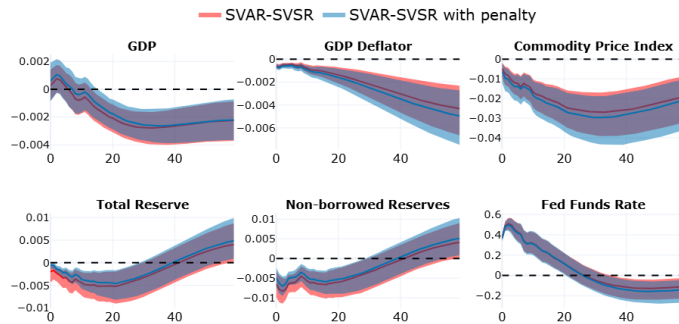
For the applications, I set the penalty to 1.2 in the elasticity-bound and narrative-restriction cases, and to 2.0 in the zero-restriction case. A higher penalty is feasible under zero restrictions because identification is already tight, so inference does not depend strongly on the threshold. In elasticity and narrative cases, I adopt a lower penalty because a high threshold yields an insufficient number of accepted draws and slows the sampler.

Figure 4 compares impulse responses from SVAR-SVSR with (blue) and without (red) the penalty function across three applications. In the elasticity-bound case (panel a), the penalty narrows the credible intervals for global activity responses to oil-specific demand and aggregate demand shocks, but the median responses remain unchanged. In the narrative-restriction case (panel b), the penalty tightens the intervals for total reserves and non-borrowed reserves, again without shifting the medians. In the zero-restriction case (panel c), the penalty has virtually no effect on medians or intervals, except for a slight drop in uncertainty around real interest rates.

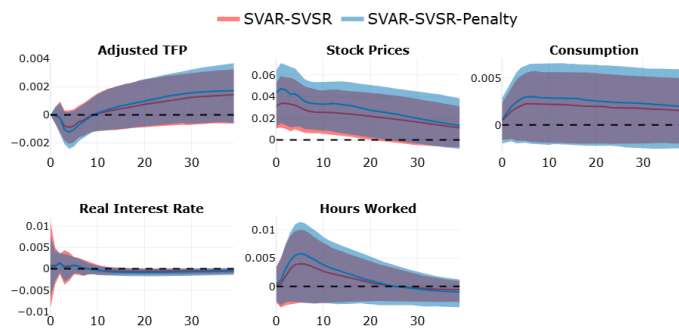
Overall, the penalty does not fully restore rotation invariance of the prior on structural variances. It reduces uncertainty only modestly and leaves the impulse responses almost identical to those from SVAR-SVSR



(a) Impulse response comparisons of SVAR-SVSR with penalty function in elasticity-bound case.



(b) Impulse response comparisons of SVAR-SVSR with penalty function in narrative-restriction case.



(c) Impulse response comparisons of SVAR-SVSR with penalty function in zero-restriction case.

**Figure 4:** Red corresponds to SVAR-SVSR without penalty function, and blue corresponds to SVAR-SVSR with penalty function. All models include heteroskedasticity with predefined regimes used in previous sections.

without the penalty. This evidence shows that SVAR-SVSR remains robust in practice, even when the prior breaks rotation invariance.

## 6 Conclusion

I develop a Bayesian SVAR with stochastic volatility and sign restrictions (SVAR–SVSR) that integrates heteroskedasticity with sign-based identification in a single coherent framework. I restore rotation invariance of the likelihood by rotating the contemporaneous matrix and the regime-specific variances with the same orthogonal transformation. As a result, the sign restrictions—not accidental likelihood tilt across rotations—drive posterior inference. I implement the method in structural space and enforce signs on the full IRFs across horizons.

The empirical applications show clear gains. In the oil market with elasticity bounds, SVAR–SVSR tracks benchmark responses but tightens credible intervals and delivers a more intuitive path for global activity after oil-specific demand shocks. In the monetary case with narrative restrictions, the model produces sharper declines in reserves and commodity prices and a clearer contraction in output. In the optimism-shock application with zero restrictions, responses cluster near zero and credible intervals shrink, confirming earlier evidence of no meaningful expansionary effects.

I next compare two rotation schemes. Rotating only the contemporaneous matrix  $A_0$ —which breaks rotation invariance under heteroskedasticity—keeps intervals wide. Jointly rotating  $A_0$  and the structural variance matrices  $\{\Lambda_m\}$  preserves the heteroskedastic likelihood and tightens bands. The gains are largest in the sign+narrative+heteroskedastic case and smaller, though still noticeable at short horizons, in the elasticity-bound and sign-zero cases.

I also test a penalty that encourages near-diagonality of rotated variance matrices. The penalty trims bands modestly in a few places but leaves medians essentially unchanged. The main conclusions do not depend on this device: the data—through heteroskedastic likelihood information—and the economic restrictions—through signs, narratives, elasticities, and zeros—do the heavy lifting.

The framework has limits. Priors on diagonal variance matrices are not rotation-invariant; the penalty only approximates that property and introduces tuning. Identification weakens when regime separation is small or misaligned with the shocks of interest. Tight restrictions raise computational cost.

Overall, SVAR–SVSR provides a practical and stable way to blend heteroskedasticity with sign restrictions.

By restoring rotation invariance and imposing economically meaningful IRFs across horizons, the method tightens credible intervals and yields more robust conclusions for applied macroeconomic analysis.

## References

- Antolín-Díaz, J. and Rubio-Ramírez, J. F. (2018). Narrative sign restrictions for svars. *American Economic Review*, 108(10):2802–29.
- Arias, J. E., Rubio-Ramirez, J. F., Shin, M., and Waggoner, D. F. (2024). Inference Based on Time-Varying SVARs Identified with Sign Restrictions. Working Papers 24-05, Federal Reserve Bank of Philadelphia.
- Arias, J. E., Rubio-Ramírez, J. F., and Waggoner, D. F. (2018). Inference based on structural vector autoregressions identified with sign and zero restrictions: Theory and applications. *Econometrica*, 86(2):685–720.
- Baumeister, C. and Hamilton, J. D. (2015). Sign restrictions, structural vector autoregressions, and useful prior information. *Econometrica*, 83(5):1963 – 1999. Cited by: 186.
- Braun, R. (2023). The importance of supply and demand for oil prices: evidence from non-gaussianity. *Quantitative Economics*, 14(4):1163–1198.
- Brunnermeier, M., Palia, D., Sastry, K. A., and Sims, C. A. (2021). Feedbacks: Financial markets and economic activity. *American Economic Review*, 111(6):1845–79.
- Carriero, A., Marcellino, M., and Tornese, T. (2024). Blended identification in structural vars. *Journal of Monetary Economics*, 146:103581.
- Clark, T. E. (2011). Real-time density forecasts from bayesian vector autoregressions with stochastic volatility. *Journal of Business & Economic Statistics*, 29(3):327–341.
- Kilian, L. and Murphy, D. P. (2012). Why agnostic sign restrictions are not enough: Understanding the dynamics of oil market var models. *Journal of the European Economic Association*, 10(5):1166–1188.
- Lanne, M. and Luoto, J. (2020). Identification of economic shocks by inequality constraints in bayesian structural vector autoregression. *Oxford Bulletin of Economics and Statistics*, 82(2):425–452.
- Lanne, M., Lütkepohl, H., and Maciejowska, K. (2010). Structural vector autoregressions with markov switching. *Journal of Economic Dynamics and Control*, 34(2):121–131.

- Lewis, D. J. (2021). Identifying shocks via time-varying volatility. *The Review of Economic Studies*, 88(6):3086–3124.
- Lütkepohl, H. and Netšunajev, A. (2014). Disentangling demand and supply shocks in the crude oil market: How to check sign restrictions in structural vars. *Journal of Applied Econometrics*, 29(3):479–496.
- Mountford, A. and Uhlig, H. (2009). What are the effects of fiscal policy shocks? *Journal of Applied Econometrics*, 24(6):960–992.
- Rigobon, R. (2003). Identification through heteroskedasticity. *Review of Economics and Statistics*, 85(4):777 – 792. Cited by: 459.
- Rubio-Ramírez, J. F., Waggoner, D. F., and Zha, T. (2010). Structural vector autoregressions: Theory of identification and algorithms for inference. *The Review of Economic Studies*, 77(2):665–696.
- Sims, C. A. (2020). Svar identification through heteroskedasticity with misspecified regimes. Unpublished manuscript.
- Sims, C. A. and Zha, T. (2006). Were there regime switches in u.s. monetary policy? *American Economic Review*, 96(1):54–81.
- Uhlig, H. (2005). What are the effects of monetary policy on output? results from an agnostic identification procedure. *Journal of Monetary Economics*, 52(2):381–419.
- Wolf, C. K. (2020). Svar (mis)identification and the real effects of monetary policy shocks. *American Economic Journal: Macroeconomics*, 12(4):1–32.

## A Distribution of $\epsilon_t$

Imposing heteroskedasticity on the structural variance matrices helps capture time-varying volatility across regimes, but it does not account for isolated, large shocks—such as those observed during the Covid-19 pandemic or the collapse of Lehman Brothers—that can severely distort inference in Bayesian VARs. These extreme events are often too heavy-tailed to be accommodated by a standard Gaussian framework.

To address this limitation, [Brunnermeier et al. \(2021\)](#) propose modeling structural shocks as a scale mixture of Normals, which leads to a Student- $t$  distribution for each shock component. Each structural shock  $\epsilon_{i,t}$  is drawn as:

$$\epsilon_{i,t} \sim \mathcal{N}(0, \lambda_{i,m(t)} \xi_{i,t}) \quad (6)$$

$$\xi_{i,t} \sim \text{Inverse-Gamma}(\text{shape} = \alpha/2, \text{rate} = 2/\alpha), \quad (7)$$

where  $\lambda_{i,m(t)}$  captures regime-specific volatility and  $\xi_{i,t}$  introduces additional, idiosyncratic variance at the observation level.

The random scaling term  $\xi_{i,t}$  allows the model to flexibly respond to occasional outliers without distorting the overall variance structure. It captures high-frequency, uncorrelated noise that may spike temporarily due to rare but influential events. Following [Brunnermeier et al. \(2021\)](#), I set  $\alpha = 5.7$ , which implies that the probability of observing a six-standard-deviation shock is roughly 200,000 times higher than under a Gaussian distribution—making the model far more robust to tail risk.

## B Posterior sampling method and computational details

### B.1 Parameter Blocks and Marginal Likelihood

This appendix outlines the details of the Gibbs sampling algorithm based on the framework in [Brunnermeier et al. \(2021\)](#). The parameter space is divided into three blocks:

$$1. \theta_1 = \{A_0, (\Lambda_m)_{m=1}^M\}$$

$$2. \theta_2 = \{(A_i)_{i=1}^P, (\epsilon_{i,t})_{i,t=1}^{n,T}\}$$

$$3. \theta_3 = \{(\xi_{i,t})_{i,t=1}^{n,T}\}$$

Starting from the structural VAR equation in (4) and the Student- $t$  error specification in equation (4), I write the regression equation for the  $i$ th equation as:

$$\Upsilon((A_0)_i)' = X(A_+)_i + E_i, \quad (8)$$

where  $\Upsilon$  is a  $T \times n$  matrix stacking all dependent variables on the left-hand side,  $(A_0)_i$  denotes the  $i$ th row of the contemporaneous matrix  $A_0$ , and  $X$  is the matrix of regressors (including lags and the constant). The row vector  $(A_+)_i$  contains the coefficients of the  $i$ th equation, and  $E_i$  collects the residuals  $\epsilon_{i,t}$  across all  $t$ .

To incorporate prior information via dummy observations, I augment the data as:

$$\tilde{\Upsilon}((A_0)_i)' = \tilde{X}(A_+)_i + E_i, \quad (9)$$

where  $\tilde{\Upsilon}$  and  $\tilde{X}$  denote the observed data matrices, stacked with the corresponding dummy observations when such priors are imposed.

To standardize the residuals, I rescale both sides of equation (9) by two diagonal matrices:  $\mathcal{E}_i$ , whose diagonal entries are  $\sqrt{\xi_{i,t}}$ , and  $\Lambda_i$ , whose diagonal entries are  $\sqrt{\lambda_{i,t}}$ . This transforms the model into:

$$\Lambda_i \mathcal{E}_i \tilde{\Upsilon}((A_0)_i)' = \Lambda_i \mathcal{E}_i \tilde{X}(A_+)_i + \Lambda_i \mathcal{E}_i E_i. \quad (10)$$

This transformation ensures that the residual term  $\Lambda_i \mathcal{E}_i E_i$  is approximately standard Normal.

From equation (10), the unnormalized posterior for the structural parameters can be written as:

$$P[\Upsilon_t | \Upsilon_0, A_+, \theta_1, \theta_3] \cdot P[\theta_1], \quad (11)$$

where the first term represents the likelihood conditional on the data and the latent scale factors  $\xi_{i,t}$ , and the second term is the prior on  $\theta_1$ . In practice, this posterior is sampled sequentially over the three blocks  $\theta_1, \theta_2, \theta_3$  using Gibbs steps, with a Metropolis–Hastings step embedded for the rotated  $A_0$  draws if sign restrictions or heteroskedasticity-based identification are imposed.

## B.2 Gibbs Sampling Algorithm for the SVAR with Stochastic Volatility (SVAR-SV)

1. **Initialization.** Initialize the parameter vector  $x_0$  for the first block  $\theta_1 = \{A_0, (\Lambda_m)_{m=1}^M\}$  at its posterior mode. Estimate the inverse Hessian matrix  $H$  by numerically maximizing the unnormalized log-posterior in equation (11). Discard the first 1,000 iterations as burn-in to ensure convergence to the posterior distribution.
2. **Metropolis–Hastings Step.** Draw a proposal  $x^*$  from a multivariate normal distribution with mean  $x_{j-1}$  and variance  $c \cdot H$ , where  $c = 0.1$  is a scaling constant chosen to target an acceptance rate of approximately 30%. Update the Markov chain using:

$$x_j = \begin{cases} x^*, & \text{with probability } \alpha^j \\ x_{j-1}, & \text{with probability } 1 - \alpha^j \end{cases}$$

where the Metropolis–Hastings acceptance probability is

$$\alpha^j = \min \left\{ 1, \frac{P[Y_t | Y_0, A_+, x^*, \theta_3] \cdot P[x^*]}{P[Y_t | Y_0, A_+, x_{j-1}, \theta_3] \cdot P[x_{j-1}]} \right\}.$$

3. **Draw Structural and Reduced-Form Coefficients.** From  $x_j$ , extract the current posterior draws of  $A_0^j$  and  $\{\Lambda_m^j\}_{m=1}^M$ . Then compute the conditional posterior for the  $i$ th row of  $A_+$  as:

$$(A_+)_i^j = (\hat{X}' \hat{X})^{-1} \hat{X}' \hat{Y},$$

where  $\hat{X} := \Lambda_i^j \mathcal{E}_i^{j-1} \tilde{X}$  and  $\hat{Y} := \Lambda_i^j \mathcal{E}_i^{j-1} \tilde{Y}$ .

Using these, compute the standardized residuals:

$$U_i^j = (\mathcal{E}_i^{j-1})^{-1} (\hat{Y} - \hat{X} (A_+)_i^j),$$

where  $u_{i,t} := \epsilon_{i,t} / \lambda_{i,t}$  is the standardized structural shock.

4. **Draw Latent Scale Parameters.** Draw the posterior values  $\xi_{i,t}^j$  from an inverse-gamma distribution conditional on  $u_{i,t}^j$ , with shape parameter  $\alpha/2 = 5.7/2$  and rate parameter equal to 1.

5. **Iterate Inner Loop.** Increment  $j \rightarrow j + 1$  and repeat Steps 2–4 until  $j = 100$ .
6. **Store Outer Draw.** Save the draw at  $j = 10$  as the  $k$ th posterior draw, reset  $j = 2$ , and repeat Steps 1–5. Stop when  $k = 1000$ .

For additional implementation details, including tuning, convergence diagnostics, and identification issues, see [Brunnermeier et al. \(2021\)](#).

## C Additional Figures

### C.1 Elasticity-Bound SVAR-SVSR: With and Without Variance Rotation

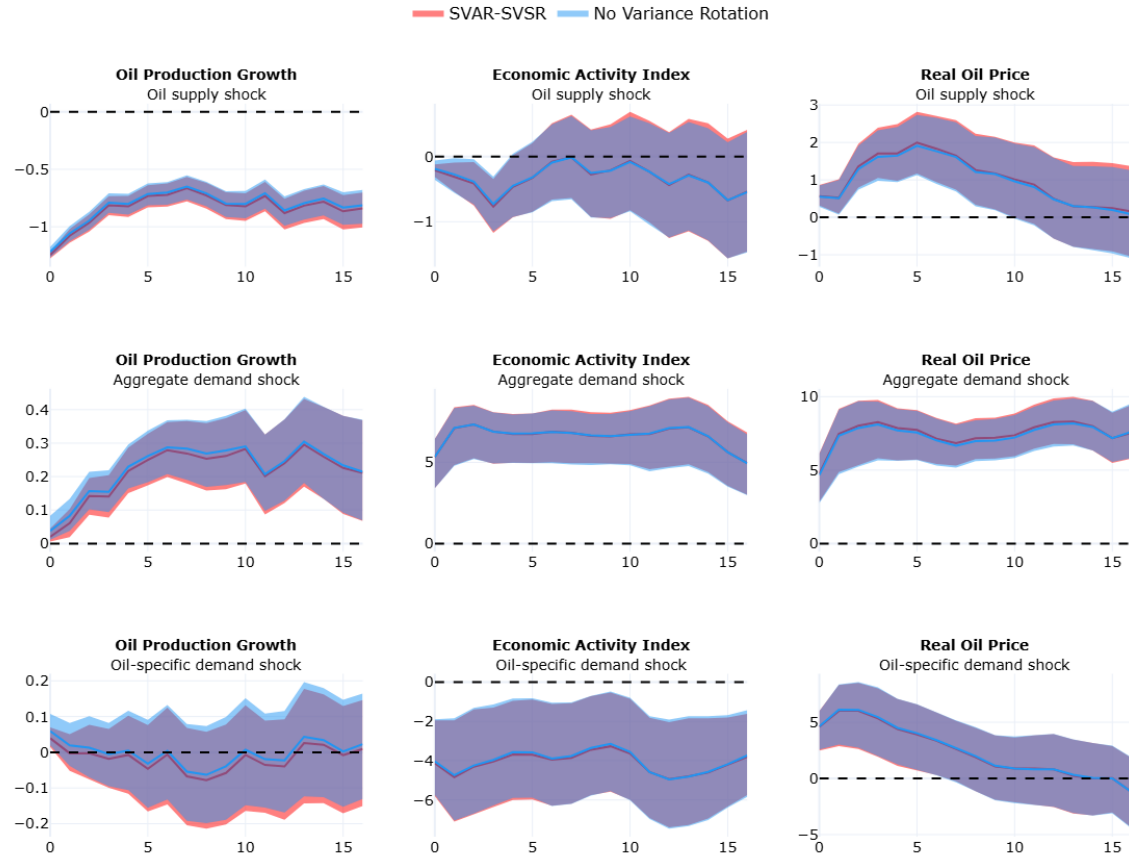


**Figure 5:** Impulse responses from SVAR-SVSR with and without variance rotation.

**Notes:** SVAR-SVSR (red) denotes the heteroskedastic model with variance rotation, while No Variance Rotation (blue) shows the same model estimated without rotating  $\lambda_{m(t)}$ . The predefined regimes are January 1971–December 1989, January 1990–December 2007, and January 2008–December 2015.

## C.2 Narrative SVAR-SVSR: With and Without Variance Rotation

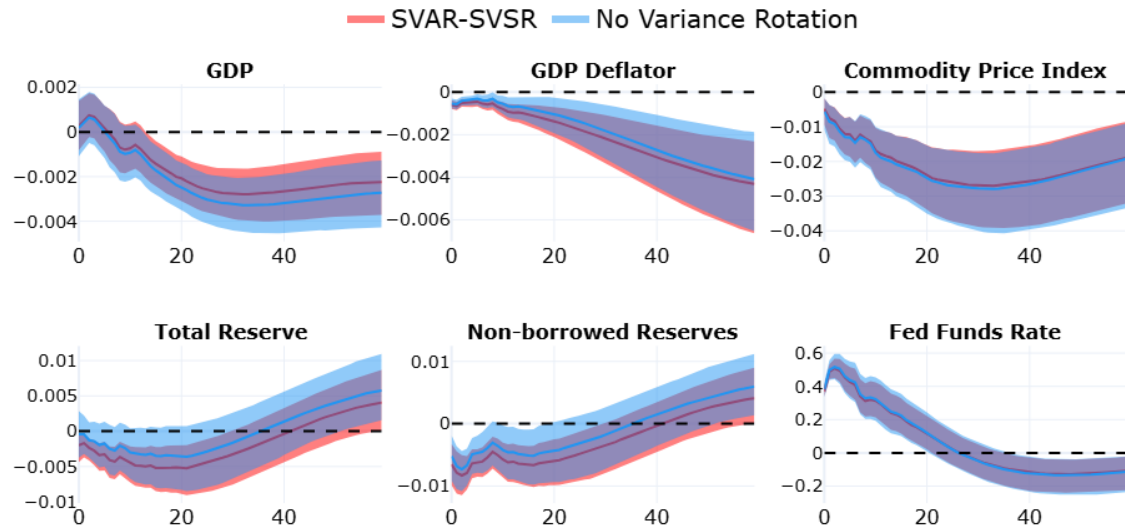


**Figure 6:** Impulse responses from SVAR-SVSR with and without variance rotation.

**Notes:** SVAR-SVSR (red) denotes the heteroskedastic model with variance rotation, while No Variance Rotation (blue) shows the same model estimated without rotating  $\lambda_{m(t)}$ . The predefined regimes are January 1965–December 1972, January 1973–September 1979, October 1979–December 1982, January 1983–December 1989, and January 1990–November 2007.

### C.3 Zero SVAR-SVSR: With and Without Variance Rotation

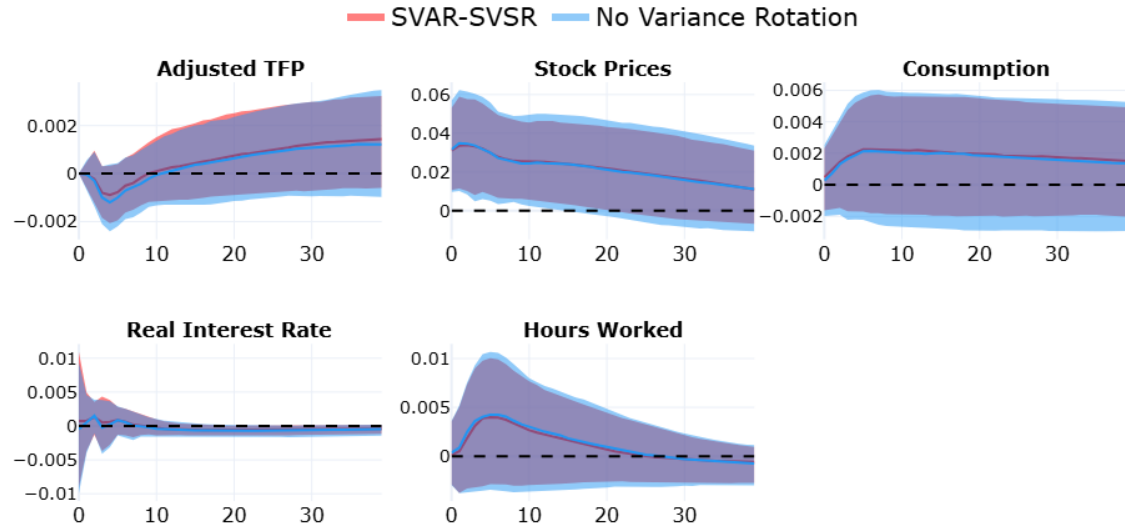


**Figure 7:** Impulse responses from SVAR-SVSR with and without variance rotation.

**Notes:** SVAR-SVSR (red) denotes the heteroskedastic model with variance rotation, while No Variance Rotation (blue) shows the same model estimated without rotating  $\lambda_{m(t)}$ . The predefined regimes are Q1 1955–Q4 1972, Q1 1973–Q4 1989, Q1 1990–Q4 2007, and Q1 2008–Q4 2010.